Computers and Concrete, Vol. 7, No. 5 (2010) 437-453
DOI: http://dx.doi.org/10.12989/cac.2010.7.5.437

Nonlinear finite element analysis of effective CFRP bonding length and strain distribution along concrete-CFRP interface

Ali Baran Doǧan*[1] and Özgür Anil[2]

[1]*MITENG Engineering Inc., Eski Guvercinlik Yolu, Gazi Mah., Ankara, Turkey, 06560*
[2]*Department of Civil Engineering, Gazi University, Maltepe, Ankara, Turkey, 06570*

(Received October 1, 2009, Accepted April 16, 2010)

Abstract. CFRP has been widely used for strengthening reinforced concrete members in last decade. The strain transfer mechanism from concrete face to CFRP is a key factor for rigidity, ductility, energy dissipation and failure modes of concrete members. For these reasons, determination of the effective CFRP bonding length is the most crucial step to achieve effective and economical strengthening. In this paper, generalizations are made on effective bonding length by increasing the amount of test data. For this purpose, ANSYS software is employed, and an experimentally verified nonlinear finite element model is prepared. Special contact elements are utilized along the concrete-CFRP strip interface for investigating stress distribution, load-displacement behavior, and effective bonding length. Then results are compared with the experimental results. The finite element model found consistent results with the experimental findings.

Keywords: effective CFRP length; nonlinear finite element analysis; CFRP-concrete bonding.

1. Introduction

Increasing needs for rehabilitation of engineering structures have resulted in numerous researches around the world for many years. Mechanical and environmental factors such as high load levels, corrosion, chemical effects that reinforced concrete structure can face during its service life prevent the structure from reaching its design performance.

There are many techniques that are used for strengthening reinforced concrete members such as adding steel plates, adding additional reinforcement to the cross-section, adding external steel plates. Among the methods, adding external steel plate is a general practice worldwide. However, maintenance, transportation difficulties, additional dead load due to its weight and its sensitivity to corrosion are general disadvantages of this method. Because of these drawbacks, use of CFRP (Carbon Fiber Reinforced Polymer) has started to replace the older methods. CFRP is a composite material with high rigidity and strength. Moreover, its low weight and resistance to external negative effects provide important advantages. Thus, number of analytical and experimental researches on FRP reinforcement has been increasing in past recent years. These researches generally focus on strain distribution along concrete-CFRP interface, concrete failure modes, crack behavior and effective bonding length (Yao *et al*. 2005, Yang *et al*. 2003, Lu *et al*. 2006, Camata *et al*. 2007, Yang *et al*. 2004, Yao and Teng

* Corresponding author, MSc., Civil Engineer, E-mail: alibarandogan@yahoo.com

2007, Teng and Yao 2007, Sharma *et al*. 2006, Lu *et al*. 2005, Yuan *et al*. 2005, Täljsten 1997, Smith and Teng 2001, Teng *et al*. 2002, Anil and Belgin 2008, Guatam and Matsumoto 2009, Yang *et al*. 2009, Schilde and Seim 2007, Pham *et al*. 2006, Pham and Al-Mahaidi 2007, Garden *et al*. 2007).

The failure mode emerges as one of the most important factor for the success of reinforcement. When the experimental studies in the literature are surveyed, three modes of failure are observed for the concrete structures strengthened with CFRP. The observed failures are debonding of concrete from CFRP, epoxy failure due to exceeding shear strength of adhesive concrete interface, and rupture of CFRP. As CFRP has very high axial tension strength, rupture is seen very rarely. This failure mode implies that whole capacity of the CFRP is used. In most cases, CFRP debonds from the concrete surface, or the adhesive concrete interface reaches its shear strength capacity and fails before the CFRP rupture. The most frequently seen mode of failure is debonding of CFRP strip together with a thin concrete layer just a couple of millimeters above the contact surface. This failure mode points out the importance of identifying the effective bonding length for preventing premature debonding of CFRP from concrete surface to make a sound and economical design. Thus, academic work on this subject is gaining importance.

In recent literature, studies covering computer modeling of interface debonding with different parameters investigate the conformity of finite element results to experimental findings using different approaches for crack behavior and concrete-FRP interface interaction (Yao *et al*. 2005, Yang *et al*. 2003, Lu *et al*. 2006, Camata *et al*. 2007, Yang *et al*. 2004, Lu *et al*. 2005, Teng *et al*. 2002, Guatam and Matsumoto 2009, Yang *et al*. 2009, Schilde and Seim 2007, Pham *et al*. 2006).

Studies focusing on different crack models, bond-slip characteristics and interfacial stresses point out the importance of interface behavior on constructing a correct finite element model (Lu *et al*. 2006, Lu *et al*. 2005, Teng *et al*. 2002, Guatam and Matsumoto 2009, Pham *et al*. 2006). Considering the previous findings concerning the effect of different parameters on concrete-plate interface behavior, some studies were aimed to constitute design criteria and predictive models for beam strengthening by relating some well-know beam parameters to failure loads (Teng and Yao 2007, Sharma *et al*. 2006, Smith and Teng 2001).

The number of analytical works being low compared to experimental researches, there is not a generalized approach for finite element modeling of CFRP-concrete interaction. This paper intends to construct a simplified finite element model, which is in good harmony with real behavior. In order to achieve this, finite element analyses are carried out for beams taken from the experimental study realized by Anil and Belgin (2008), which contains strain and load displacement behavior of CFRP sheets bonded to concrete. ANSYS software is utilized for finite element modeling purposes. ANSYS being widely used in academic literature has special finite element types for modeling concrete-FRP interface with material nonlinearities. Finite element results are compared to experimental data for verification. This way, the weak and powerful sides of the finite element model are revealed. The interface parameters are then investigated for a certain bonding length and bonding width. After defining suitable interface contact parameters, model simulation of beams with different CFRP bonding lengths is performed to determine effective bonding length. In addition to this, load-displacement relation and interface behavior are simulated for beams without experiment. The amount of test data being increased this way, it became possible to gain a deeper insight into the effective CFRP length which sustains shear strains.

2. Experimental study

2.1 Test specimens and materials

Sixteen notched concrete beams were casted and tested under monotonic loading. Experimental program details are given in Anil and Belgin (2008). No reinforcement was used in the beams. The geometrical dimensions of the test specimens are given in Fig. 1. The beams were casted with a 20 mm wide and 50 mm deep notch to evaluate the effect of cracks on the stress distribution between CFRP and concrete. The notch was placed at the midpoint of the span, on the symmetry axis. The cross-section of the concrete beams was 150×200 mm and the span length between the supports was 1200 mm. The load was applied monotonically with a four point loading arrangement.

The properties of the test specimens are given in Table 1. Sixteen beams were casted (2×4×2) with two different width and four different CFRP bonding lengths. Concrete compressive strength was chosen to be 15 MPa and 25 MPa. The compressive strengths of the test beams found from standard cylindrical compression test are given in Table 1. 50 mm and 100 mm wide CFRP strips were used with 120 mm, 180 mm, 240 mm, and 300 mm bonding lengths.

The bonding procedure of CFRP's was carried out according to CFRP and epoxy manufacturer's application guide. For strengthening, unidirectional CFRP named Sikawrap 230C was used together with two component epoxy Sikadur 330. The properties of these materials are given in Table 2. These values are supplied by the manufacturer.

Before bonding CFRP members on the concrete surface, special consideration was given to beam surface preparation. Bottom surface of the beam web was roughed by a mechanical grinding machine until the aggregate was exposed and the surface was vacuumed to remove loose particles and dust. After a smooth and dust free surface was obtained, the epoxy resin was mixed as per manufacturer's instructions. Mixing was carried out in a metal container until having a uniform

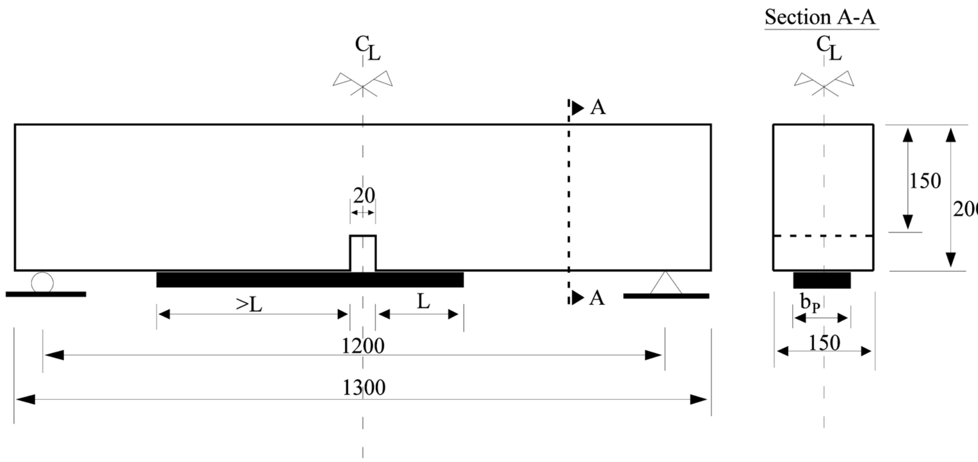

Notes : L : Bonding length of CFRP = 120, 180, 240 and 300 mm

b_p : CFRP width = 50 and 100 mm

Dimensions in mm.

Fig. 1 Details of test specimens

Table 1 Properties of specimens

Specimen #	Average compression strength of concrete f_C (MPa)	CFRP strip width b_P (mm)	CFRP strip bonding length L (mm)
1	15.2	50	120
2	14.8		180
3	14.4		240
4	15.6		300
5	15.8	100	120
6	14.2		180
7	14.7		240
8	15.3		300
9	25.0	50	120
10	26.0		180
11	24.0		240
12	25.2		300
13	24.8	100	120
14	24.4		180
15	25.6		240
16	25.0		300

Table 2 Properties of CFRP and resin

Properties of CFRP	Remarks of CFRP*
Construction	Warp : Carbon fibers (99% of total areal weight) Weft : Thermoplastic heat-set fibers (1% of total areal weight)
Areal weight (g/m^2)	220±10
Density (g/m^3)	1.78×10^{-6}
Thickness (mm)	0.12
Tensile strength (MPa)	4100
Elastic modulus (MPa)	231000
Ultimate tensile strain (%)	1.7%
Properties of resin	Remarks of resin*
Tensile strength (MPa)	30
Elastic modulus (MPa)	3800

*These values are supplied by the manufacturer

color. The prepared epoxy resin (Sikadur 330) was applied to the surface of the concrete where the CFRP will be bonded. Then the Sikawrap230C was laid on to the epoxy resin and pressed thoroughly to assure absorption of the resin by fiber material and to obtain bubble free interface between CFRP and concrete. Finally, CFRP is covered with another layer of epoxy resin with a thickness of 0.5 mm for protection. Temperature during the application was 20±2°C. The beams were tested after 14 days.

2.2 Experimental setup

The tests were carried out in a closed frame with a capacity of 400 kN. Monotonic load was applied with a 300 kN capacity hydraulic jack. Experimental and measurement setups are given in

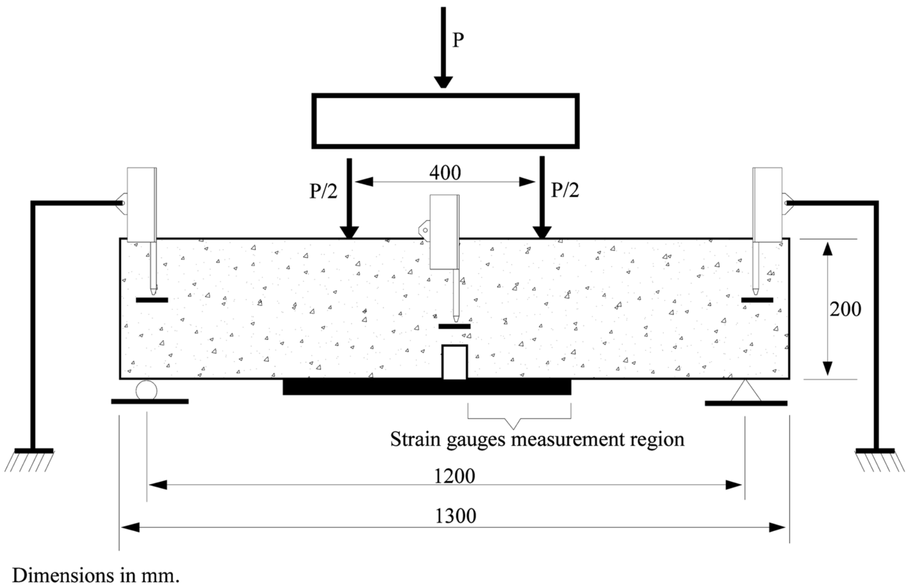

(a) Schematic view of test setup and instrumentations

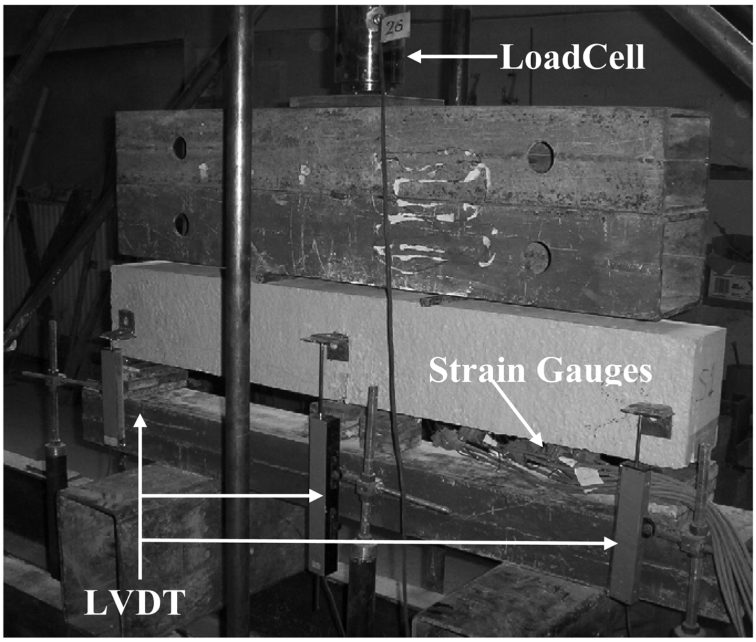

(b) Photograph of test setup

Fig. 2 Test setup and instrumentations

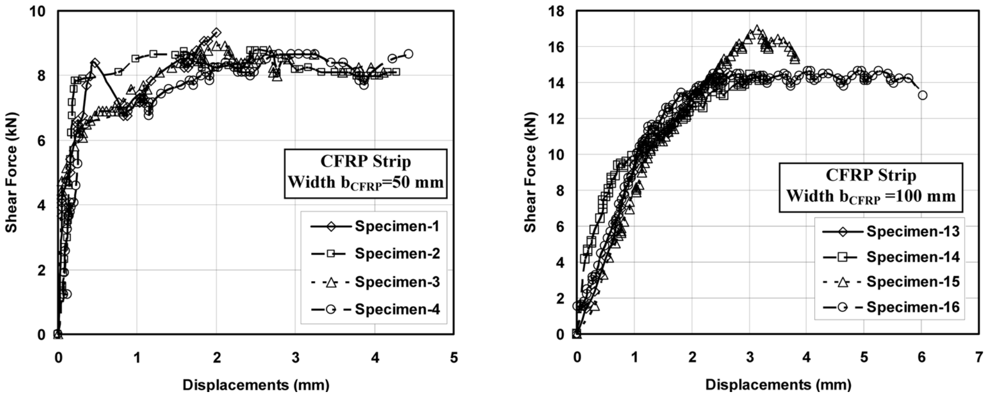

Fig. 3 Examples of load-displacements graphs of the specimens

Fig. 2. Load controlled displacement was applied to the beams. In all specimens the ratio of shear span length (a = 400 mm) to the effective depth (d = 200 mm) was (a/d = 2) identical. A load-cell with a capacity of 400 kN was used for measuring applied load during the experiments. The vertical displacements of the supports and the midpoint deflections were measured by displacement transducers (Linear Variable Differential Transformers (LVDT)). Beam midpoint net displacements due to bending were calculated using the vertical displacements of the supports. The tests were carried out observing the load-midpoint displacement graphic sketched simultaneously on the monitor. Load was increased until the beams failed. Strain measurements are taken along CFRP strips up to notch for measuring stress distribution at concrete-CFRP interface (Fig. 2).

2.3 Observed behavior and failure modes of specimens

A typical example of the load-displacement graphics of the test specimens are given in Fig. 3. The main parameter affecting the ultimate load capacity of the specimens is found to be the CFRP strip width when the load-displacement graphics are examined. It is noted that the CFRP strip bonding length and the compressive strength of concrete hardly had a contribution on the ultimate load capacity of the specimens.

Two types of failure modes are observed during the experiments. The first mode is debonding of CFRP with concrete layer just a couple of millimeters above from the contact surface and the second one is failure of the adhesive concrete interface. Observing the specimens, it can be seen that the thickness of concrete layer which is debonded from the surface together with the CFRP strip decreases and becomes uniform as CFRP strip length increases. This thickness increases with increasing CFRP strip width. In order to evaluate the changes in strain distribution during loading, strain values of five different load levels are given in Fig. 4.

3. Finite element modeling

ANSYS modeling, which forms the backbone of this study, consists of three parts. In the first part, some specimens are selected from Table 1 for finite element modeling. In this selection, beams with different concrete compressive strength and CFRP strip width are considered to represent the

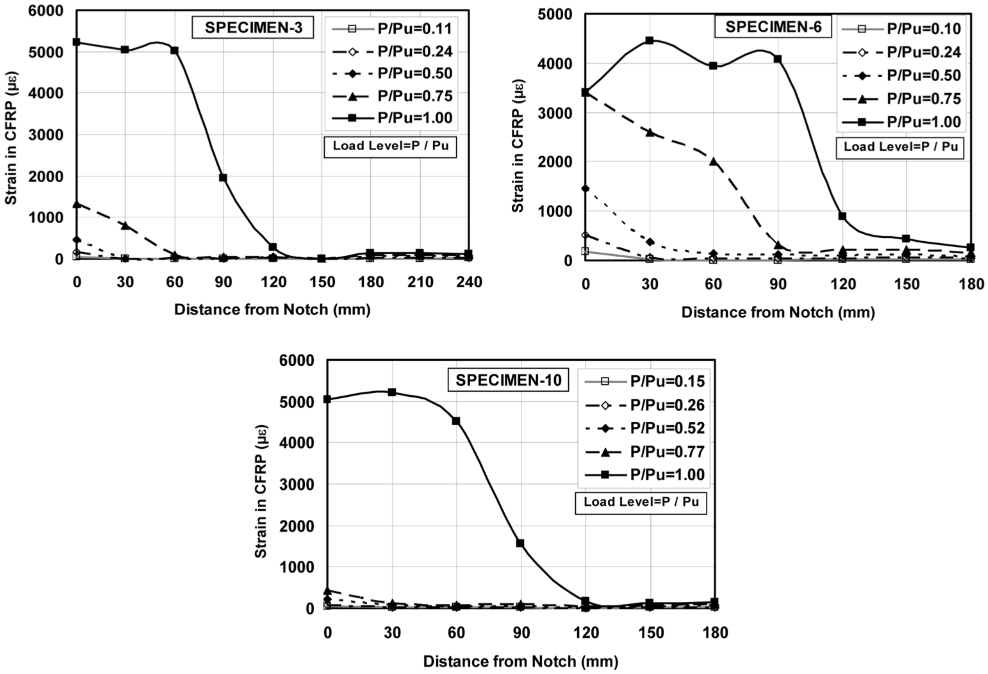

Fig. 4 Examples of strain distribution graphs of the specimens

experiment parameters better. ANSYS finite element model results are compared to experimental findings to check the accuracy and applicability of the finite element model.

In the second part of the study, the contact surface modeling parameters are determined by trying different values for maximum interface stress (τ_{MAX}) within various finite element analyses. Using these contact surface parameters to represent the interface behavior, CFRP bond length is increased progressively on verified computer models to investigate strain distribution generated between concrete and CFRP strip.

The third part includes modeling Specimens 13, 14, 15, and 16 with 25 MPa concrete compressive strength and 100 mm CFRP strip width using the contact surface parameters identified in the previous step. Later, analysis for beams having 360 mm and 420 mm CFRP length, for which no experiment was conducted, are implemented. The increased number of data enables to reach more accurate conclusions. Eventually, it has been possible to determine effective bonding length from the increasing number of ANSYS finite element analyses that are made for beams with and without experimental results.

3.1 Physical finite element model

Increasing the number of finite elements provides better approximations but increases the computational time considerably (ANSYS User's Manual 2005). After some limit, however, increasing the number of finite elements does not improve the analysis results and unnecessarily increases time required for solution (ANSYS User's Manual 2005, Moaveni 1999). For the sake of effectiveness, analyses are run to monitor changes in failure loads with different mesh sizes. The results are given in Fig. 5.

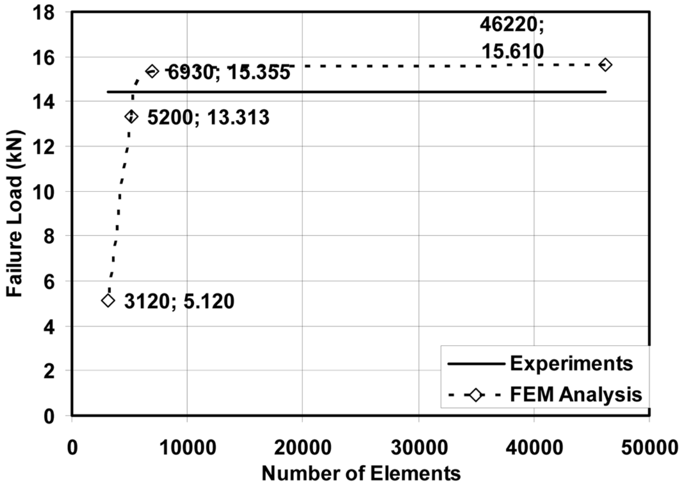

Fig. 5 Failure load and element amount

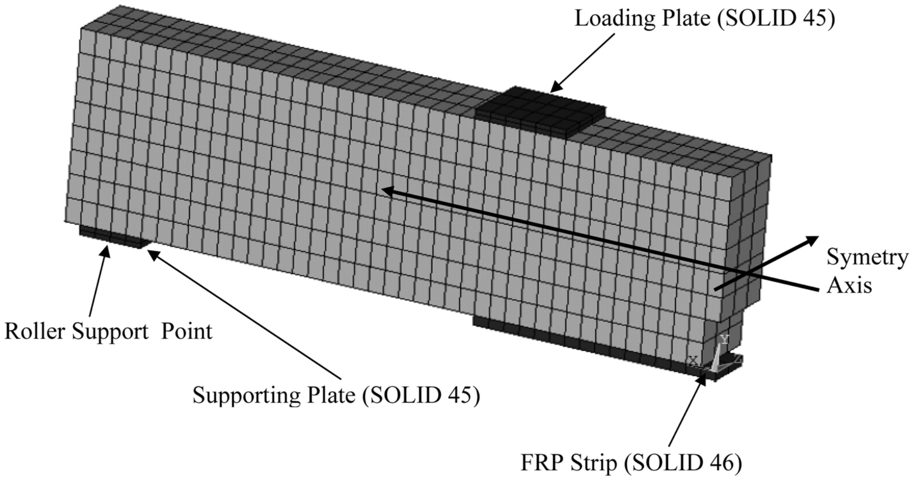

Fig. 6 Finite element model

When Fig. 5 is analyzed, it can be seen that increasing the amount of finite element beyond 6930 does not affect failure load results. When number of finite elements is decreased, problems emerging from convergence difficulties hinder the process and the solution ceases in early steps. Actually, there is a little difference between 5200 and 6930 finite elements but model with 6930 elements comprising 15×15×25 mm prismatic elements represents the beam geometry better than the model with 5200 finite elements with dimensions of 15×20×25 mm.

The geometrical restrains are taken into account in mesh dimension selection. Finite element mesh is generated with 6930 elements. Taking advantage of symmetry, only one quarter of the beams is modeled and convenient joint restrains are used in the direction perpendicular to symmetry axis. In the early steps of the analysis, formation of local cracks at support and load application points created convergence problems. This was handled by using SOLID 45 finite element (ANSYS User's Manual 2005) defined within ANSYS software and by assigning boundary conditions allowing rotation in support points. In order to prevent concrete cracks around load application point, total beam load is distributed to 4 nodes (Fig. 6).

So as to prevent abrupt changes in element dimensions, there exists a pre-defined limit in ANSYS for elements being connected to each other by their nodes. For this reason, 0.12 mm thick CFRP layer is modeled with 10 mm thickness and to compensate for this increase in cross section, its elastic modulus is modified accordingly. To ensure that its nodes are properly connected to concrete nodes, CFRP element dimension is defined as 10×15×25 mm.

Table 3 Material properties

Material	Element type	Material properties		
1	Solid65	Linear isotropic hardening		
		E_X (MPa)	2,1E+4	
		P_{RXY}	0.3	
		Multi linear isotropic hardening		
			Strain	Stress (MPa)
		1. Point	0.0003	6.7
		2. Point	0.0004	8.7
		3. Point	0.0008	15.6
		4. Point	0.001	18.3
		5. Point	0.001718	24.3
		6. Point	0.002068	25
		7. Point	0.0038	21.25
		Concrete		
		ShrCf-Op	1	
		ShrCf-Cl	1	
		UnTensSt(MPa)	3.2	
		UnCompSt(MPa)	-1	
		BiCompSt	0	
		HydroPrs	0	
		BiCompSt	0	
		UnTensSt	0	
		TenCrFac	0	
2	Solid 46	Linear isotropic		
		E_X(MPa)	2770	
		P_{RXY}	0.22	
3	Solid 45	Linear isotropic		
		E_X(MPa)	2,1E+5	
		P_{RXY}	0.3	
4	Targe170 Conta173	Linear isotropic		
		E_X(MPa)	3800	
		TAUMAX τ_{MAX} (MPa)	20	

3.2 Material models

In this study, Hognestad model for unconfined concrete is used together with William and Warnke triaxial failure surface. Concrete tension strength is taken from experiments for concrete under two point loading (Ersoy 2000) to simulate stress conditions during experiments. Regarding the behavior of concrete after cracking, it is assumed that all shear forces are transferred. In addition to this, crushing of concrete is neglected to prevent convergence problems.

For ANSYS modeling of concrete, Solid 65 element is selected. This finite element has ability to make plastic deformations, can demonstrate crushing and cracking behavior in the direction perpendicular to principal stress and comprises concrete failure criteria under triaxial loading condition. As CFRP layer is studied under indirect tension forces, only properties along fiber direction will be used. For this reason, isotropic linear elastic material model is assigned to CFRP. Solid 46 elements is selected in ANSYS software for CFRP layer assuming that the fibers are distributed uniformly within the binding material, there are no voids in the composite CFRP layer, forces act in the fiber direction and a perfect bond exists between fibers and epoxy. In order to facilitate convergence by preventing local effects in the vicinity of loading and supporting points, plates made up of totally elastic Solid 45 finite elements are used at these points. For some analysis, a contact surface between concrete and CFRP is created using special Targe 170 and Conta 172 elements (ANSYS User's Manual 2005).

Aforementioned material properties are summarized in Table 3. Investigations made on interface CFRP strain distribution for defining contact surface parameters will be presented in following sections.

3.3 Contact surface

In contact problems, variables like Coulomb friction coefficient (μ), cohesion (C), axial-shear rigidity and maximum shear force that can exist between two surfaces (τ_{MAX}), which is the most important property in this study, can be defined within ANSYS software. Shear yield of the contacting surfaces places a physical limit to how large shear stress can be transmitted. Thus, real constant τ_{MAX} is used in contact surface modeling (ANSYS User's Manual 2005).

The interaction between CFRP and concrete is different from a classic Coulomb friction model, in which mobilization of friction depends on axial compression. The maximum shear resistance between surfaces becomes the key parameter in this study because a bonded contact analysis was conducted without axial confinement. In addition to this, assuming zero friction along the interface under pure bending conditions represents the experimental results better (Guatam and Matsumoto 2009). Empirical data is suggested to be the best source for $_{MAX}$, but an upper limit is specified by Eq. (1) as; (ANSYS User's Manual 2005).

$$\tau_{MAX} = F_y \times 1/\sqrt{3} \tag{1}$$

F_y stands for axial strength of FRP material in this equation. To model the contact surface closer to real behavior, some analyses are carried out with and without contact surfaces. Distance from Notch vs. CFRP strain curve obtained without utilizing a contact surface for beam 16 is compared with strain distributions obtained by using different $_{MAX}$ values (Fig. 7). These curves suggest that strain distribution changes considerably when a contact surface is introduced. The maximum and minimum values of shear strain remains very close to each other in both cases. In effect, the most

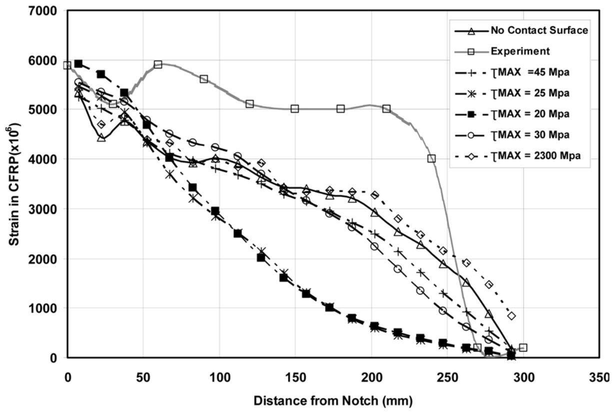

Fig. 7 Strain distribution for different interface maximum shear strength (τ_{MAX}) values for beam-16

important feature of this graph is the abrupt change in strain distribution around τ_{MAX} =25-30 MPa. This was also observed in previous studies on FRP debonding, sudden change in curvature of the strain vs. distance from notch graph corresponds to debonding just before or during the application of failure load (Lu *et al*. 2005, Täljsten 1997, Yang *et al*. 2009, Pham *et al*. 2006). However, for the current test specimens, this debonding was not explicitly observed (Anil and Belgin 2008). Contact surface analysis run on beam 16 points out that using interface shear strength (τ_{MAX}) around 20 MPa represents strain distribution just before debonding, close to real behavior.

4. Finite element modeling results

4.1 Analysis for verification of FEM model

For verification purposes, analyses are run without contact elements; that is to say, CFRP and concrete nodes are directly interconnected assuming a perfect bond. Each analysis will be viewed from below perspectives;

1. Failure load
2. Beam mid point deflection during failure
3. Stress-strain relationship
4. Maximum CFRP axial strain
5. Strain distribution along bonded CFRP length.

Comparison of analysis and test results is presented in Table 4 at which beam failure load is about 10% more than experimental results. This difference is acceptable for engineering analysis in general. However, when mid point deflections before failure are studied, it is noted that experimental values exceed computer analysis results by 56%, which means that finite element model has not been successful in predicting beam ductility.

Maximum values of CFRP shear strain are above the test results for 50 mm CFRP width but are below the test results for 100 mm wide strips. The mean difference is between 6% and 25% which stays within acceptable limits.

Table 4 Comparison of experiment and FEM results

Specimen #	FEM ultimate load (kN)	Experimental ultimate load (kN)	% Error	FEM Max. deflection (mm)	Experimental Max. deflection (mm)	% Error	FEM Max. CFRP strain	Experimental Max. CFRP strain	% Error
3	8.71	8.92	-2	2.9	4.1	-29	5500	5213	6
7	12.74	14.08	-10	2.38	3.52	-32	4269	5668	-25
11	10.53	9.32	13	2.52	3.3	-24	6573	5919	11
13	14.66	14.54	1	1.15	2.62	-56	4545	5558	-18
14	15.36	14.43	6	1.64	3.18	-48	4829	6027	-20
15	15.82	16.96	-7	2.12	3.81	-44	5039	5499	-8
16	16.43	14.62	12	2.63	6.03	-56	5349	5880	-9

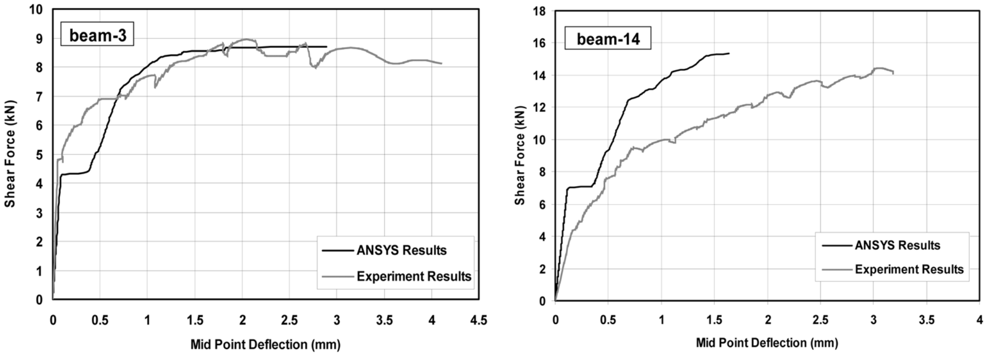

Fig. 8 Comparison of load-displacement curves

Aiming to interpret differences between the experiment and finite element model findings, their load displacement curves are compared. Some sample load-displacement curves are given in Fig. 8. Initial stiffness of ANSYS models is generally greater than the experiments. The general characteristic of load displacement curves of ANSYS models is such that they have a notable horizontal plateau portion after the end of elastic region. Load steps were held small enough during analysis to capture this behavior. In finite element analyses, dramatic rigidity changes are occurred after crack formation. As a result of this, beam behavior shifts from linear to nonlinear. The horizontal portion in load displacement curves of ANSYS analyses indicates the beginning of this rigidity change right after the cracks are formed. Limits of linear behavior in computer models are in good agreement with experimental findings.

Realistic results for ductility have not been acquired in ANSYS computer modeling. Reasons for this can be counted as abrupt nature of crack formation, complex crack distribution before ultimate load and fixed angle crack model not being able to represent crack patterns accurately (Lu *et al.* 2005, 2006). In addition to above, increasing CFRP length or width introduces some ambiguity to the model and thus increases divergence between experiment and ANSYS results.

4.2 Analysis on strain distribution along the interface

In the fixed angle crack model (FACM), the cracks form in the direction perpendicular to principal stress and their direction remains the same. As shear forces occur along the interface, to account for shear force transfer after crack formation, a coefficient between 0 and 1 is utilized. The shear stress being increased even after cracking, this fixed angle crack model does not provide satisfying results for debonding behavior which is in fact shifting of effective stress transfer zone (Lu *et al*. 2006). For this reason, a special contact surface is developed to investigate in detail the strain behavior of CFRP along concrete interface.

To determine strain distribution, CFRP bonding length is increased for constant 100 mm strip width and 25 MPa concrete compressive strength. Firstly, beams 13, 14, 15 and 16 are modeled with and without special contact surface. Then, this analysis is extended further for untested beams having 360 mm and 420 mm bonding lengths. Strain distributions for these four beams are presented in Fig. 9.

Fig. 9 points out that for short bond lengths, strain distributions do not change much, but with increasing strip length the slopes of curves change considerably. It is worth noting that use of contact surface and the increase in CFRP strip length have a little effect on maximum and minimum strain values.

The difference between shapes of strain distribution curves at two load stages, namely the time of debonding initiation and failure, resembles the difference between the analysis run with and without contact surfaces. Total applied load at these two load levels, where the sign of the slope of strain distribution curve tends to change suddenly due to debonding, are in fact very close to each other. This abrupt variation of strain distribution in these very close load levels was also observed in

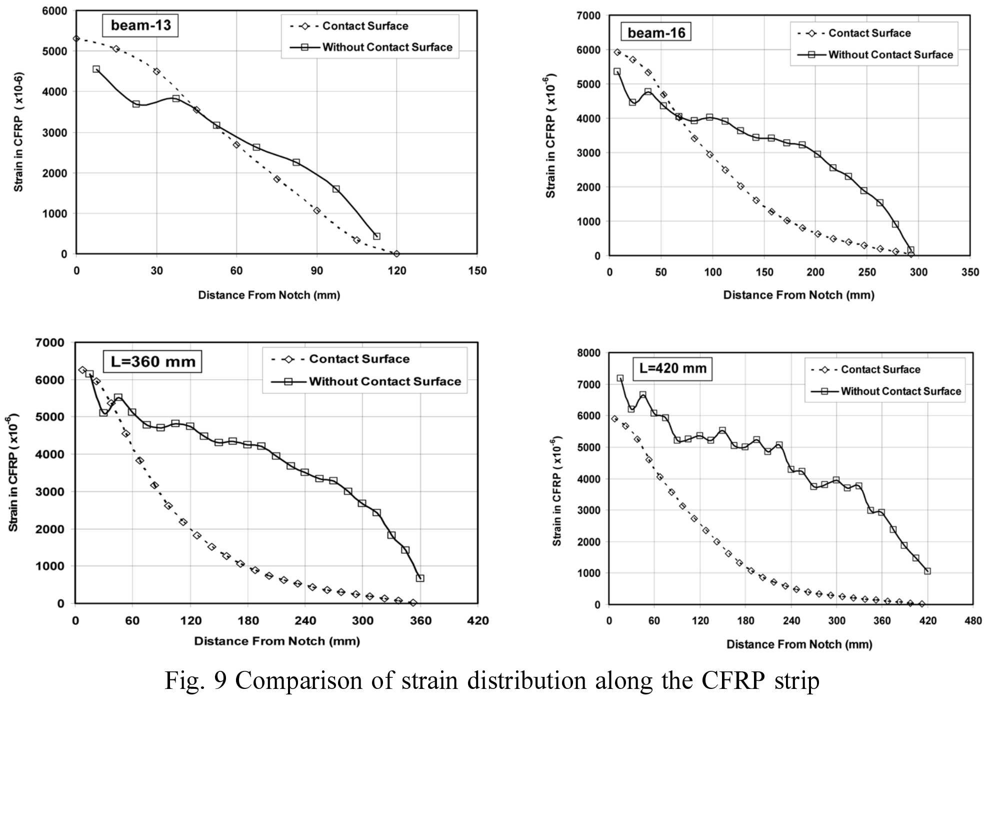

Fig. 9 Comparison of strain distribution along the CFRP strip

previous studies (Lu *et al*. 2005, Täljsten 1997, Yang *et al*. 2009, Pham *et al*. 2006).

Assigning a special contact surface between CFRP and concrete is a better approach in finite element modeling as it simulates a load level very close to cause total collapse, just before the initiation of debonding. Moreover, it disperses local strain fluctuations and provides a smooth parabolic strain distribution, which proves to ease of determination of effective bonding length.

Experimental strain graph given in Fig. 4 shows that strain values are nearly constant before the sudden drop. However, in lower loading levels, this constant part does not exist. This means that as load increases towards its ultimate value, a sudden drop occurs in strain-distance from notch graph after the constant portion, which implies debonding of CFRP from concrete surface (Sharma *et al*. 2006, Täljsten 1997, Yang *et al*. 2009). The CFRP strip length resisting the stress changes, and with the start of debonding, some variations of abrupt nature are observed. The position of this dramatic change provides an idea on the effective portion of total bonded CFRP strip length.

As bond-slip relation cannot be modeled close enough to real behavior in finite element analysis, differences in strain distributions may sometimes be more than expected (Lu *et al*. 2005). Also, inhomogeneities of concrete material and singularities because of aggregate interlock cause differences in strain values along the interface.

4.3 Effective bonding length

Strain distributions for different bonding lengths are presented in Fig. 10. When CFRP bonded length increases, far end strains quickly decrease as slope of the graph decreases. Increased strip length does not effectively resist strain. These remarks point out the existence of an effective bonding length for CFRP in ANSYS finite element model.

In order to investigate this effective length, the portion of CFRP strip which attain 90% of maximum strain is regarded as effective working length and change of this effective length versus total bonded length is plotted in Fig. 11. As can be seen in the graph, for short bonding lengths, working CFRP length is very close to total bonded length. The graph increases linearly until the working length reaches to 240 mm. After 240 mm, working CFRP length remains constant. This point is the effective bonding length after which increasing total length of CFRP strip will not

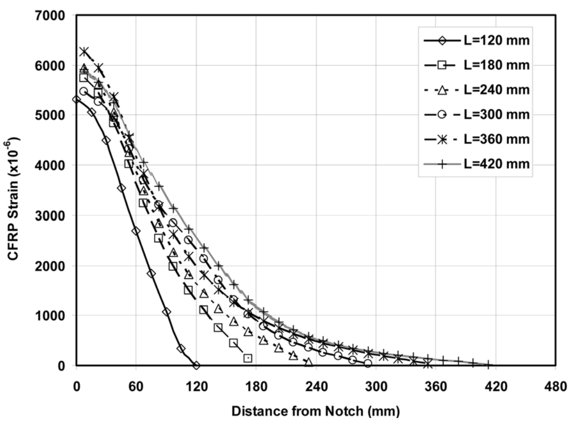

Fig. 10 Comparison of strain distribution along the interface for different bonding lengths

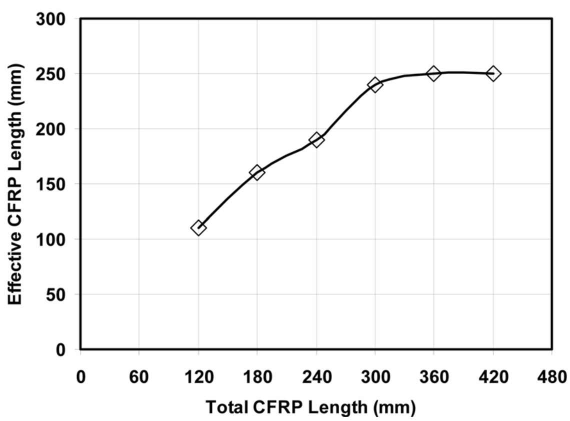

Fig. 11 Change of effective CFRP length with total bonding length

improve strain carrying capacity. Experimental results indicate that the effective bonding length is 270 mm for specimen-16, in which strain-distance from notch graph vertically drops after a constant portion.

5. Conclusions

In the scope of this study, a finite element model has been constructed and nonlinear finite element analyses of 7 experimental beams were implemented for verification purposes. These test beams were selected among the experiments conducted by Anil and Belgin (2008) for concrete beams under indirect tension with different CFRP bonding length, width and concrete compressive strength. No reinforcement was used in the beams. In order to model the concrete-CFRP interface strain distribution, contact surface analyses were run with different interface shear strength values. Comparing the strain distribution with data from previous studies, the computer model was improved. In the next stage, CFRP length was increased to monitor strain behavior along the interface while its width was kept constant. For longer bonding lengths which are not covered by the experiments, model simulation was realized and by the help of increased data, some remarks were done for effective bonding length. Findings obtained by comparing experiment and finite element results are listed below.

- In analyses done for verification, there has been an average difference of 10% between experiments and computer models for failure load. This difference rose to 20% for maximum CFRP strain. It is concluded that computer model is in accordance with experimental results.
- When load-displacement relations in ANSYS model are reviewed, the plateau portion after the end of elastic behavior can easily be noted. After cracking of concrete in ANSYS model, rigidity changes considerably and behavior becomes nonlinear. This change can be tracked on load-displacement curve. Initial rigidity, yield load, yield point displacement and in general load displacement curves of computer models are in good agreement with experimental results.
- Computer models do not satisfactorily represent midpoint deflections and ductility of test beams. It is deemed that the reason for this is the crack model used in ANSYS software. In the fixed angle crack model (FACM) which is used in the software, the cracks form in the direction perpendicular to principal stress and its direction remains the same. But when the direction of principal stresses change to form shear stress along the interface, the shear strength of cracked concrete is generally modeled with a shear transfer coefficient between 0 and 1. The shear stress being increased even after formation of cracks, this fixed angle crack model does not provide satisfying results in identifying debonding behavior which is in fact shifting of effective stress transfer zone. For this reason, a need emerged on developing a contact surface to investigate in detail the strain behavior of CFRP along concrete interface.
- In order to determine effective bonding length from strain distribution of model tests carried out by increasing CFRP strip length, it is necessary to use a smooth, parabolic shaped distribution for a state of strain immediately before debonding. This is possible by assigning special type contact surface elements defined within ANSYS and by limiting the maximum shear stress than can be sustained between CFRP and concrete.
- When no contact elements are used between concrete and CFRP nodes, maximum CFRP strain and failure load results improve, but debonding of CFRP layer can not be clearly distinguished as there is no abrupt change in interface strain distribution.

- For the purpose of defining interface strain distribution more accurately, it is necessary to define a maximum stress value (τ_{MAX}) along the interface and run contact analyses. The strain distribution obtained this way gives important information on effective bonding length.
- Using verified finite element models, the amount of data is increased by making model simulation of untested beams. Strain distribution along the concrete-CFRP interface is determined for different bonding lengths. CFRP strip length after the point where strain value falls below 10% of total strain is assumed not to sustain shear stress. CFRP strip length carrying practically all effective stress is determined.
- Working CFRP length increases linearly with increasing bonding length, but remains constant after some limit. It is revealed that after this stage, strain is not transferred effectively by CFRP even if bonding strip length is increased. It is also proven that effective bonding length is in conformity with experimental findings.

This paper includes finite element investigations to determine effective bonding length for 100 mm wide CFRP strip which is extensively used in strengthening works. For future studies, running numerous nonlinear finite element analyses by changing some modeling parameters like CFRP strip width, concrete compressive strength, width of concrete beam and stress conditions would be an important step towards determination of generalized formulas, rules and recommendations for CFRP design. Besides, effective CFRP length investigations can be extended for single shear tests, modeling the debonding behavior of concrete-CFRP interface by computer finite element analyses. A correlation between indirect tension, direct tension and experiment results can then be shaped to introduce design recommendations for CFRP strengthening of reinforced concrete beams.

References

Anil, Ö. and Belgin, Ç. (2008), "Review of bond-strength models and application on CFRP- to-concrete bonded joints across crack", *Sci. Eng. Compos. Mater.,* **15**(2), 141-158.

ANSYS (2005), *ANSYS user's manual revision 10.0*, ANSYS, Inc., Cannonsburg, Pennsylvania.

Camata, G., Spacone, E. and Zarnic, R. (2007), "Experimental and nonlinear finite element studies of RC beams strengthened with FRP plates", *Compos. Part B - Eng.*, **38**, 277-288.

Ersoy, U. (2000), *Reinforced Concrete*, METU, Ankara.

Garden, H.N., Quantrill, R.J., Hollaway, L.C., Thorne, A.M. and Parke, G.A.R. (2007), "An experimental study of the anchorage length carbon fibre composite plates used to strengthen Reinforced concrete beams", *Compos. Struct.,* **21**, 709-726.

Guatam, B.P. and Matsumoto, T. (2009), "Shear deformation and interface behavior of concrete-filled CFRP box beams", *Compos. Struct.*, **89**, 20-27.

Lu, X.Z., Teng, J.G., Ye, L.P. and Jiang, J.J. (2005), "Bond-slip models for FRP sheets/plates bonded to concrete", *Eng. Struct.*, **27**, 920-937.

Lu, X.Z., Jiang, J.J., Teng, J.G. and Ye, L.P. (2006), "Finite element simulation of debonding in FRP-to-concrete bonded joints", *Constr. Build. Mater.*, **20**, 412-424.

Moaveni, S. (1999), *Finite element analysis: theory and application with ANSYS*, Prentice-Hall, New Jersey.

Pham, H.B., Al-Mahaidi, R. and Saouma,V. (2006), "Modeling of CFRP-concrete bond using smeared and discrete cracks", *Compos. Struct.*, **75**, 145-150.

Pham, H.B. and Al-Mahaidi, R. (2007), "Modeling of CFRP concrete shear-lap test" *J. Constr. Build. Mater.,* **21**, 727-735.

Schilde, K. and Seim, W. (2007), "Experimental and numerical investigations of bond between CFRP and concrete", *Constr. Build. Mate*r., **21**, 709-726.

Sharma, S.K., Mohamed Ali, M.S., Goldar, D. and Sikdar, P.K. (2006), "Plate-concrete interfacial bond strength

of FRP and metallic plated concrete specimens", *Compos. Part B - Eng.,* **37**, 54-63.
Smith, S.T. and Teng, J.G. (2001), "Interfacial stresses in plated beams", *Eng. Struct.*, **23**, 857-871.
Täljsten, B. (1997), "Defining anchor lengths of steel and CFRP plates bonded to concrete", *Int. J. Adhes. Adhes.*, **17**, 319-327.
Teng, J.G. and Yao, J. (2007), "Plate end debonding in FRP-plated RC beams-II: strength model", *Eng. Struct.*, **29**, 2472-2486.
Teng, J.G., Zhang, J.W. and Smith, S.T. (2002), "Interfacial stresses in reinforced concrete beams bonded with a soffit plate: a finite element study", *Constr. Build. Mater.*, **16**, 1-14.
Yang, D.S., Park, S.K. and Neale, K.W. (2009), "Flexural behavior of reinforced concrete beams strengthened with prestressed carbon composites", *Compos. Struct.*, **88**, 497-508.
Yang, Q.S., Peng, X.R. and Kwan, A.K.H. (2004), "Finite element analysis of interfacial stresses in FRP-RC hybrid beams", *Mech. Res. Commun.*, **31**, 331-340.
Yang, Z.J., Chen, J.F. and Proverbs, D. (2003), "Finite element modeling of concrete cover separation failure in FRP plated RC beams", *Constr. Build. Mater.*, **17**, 3-13.
Yao, J., Teng, J.G. and Chen, J.F.M. (2005), "Experimental study on FRP-to-concrete bonded joints", *Compos. Part B - Eng.,* **36**, 99-113.
Yao, J. and Teng, J.G. (2007), "Plate end debonding in FRP-plated RC beams – I: Experiments", *Eng. Struct.*, **29**, 2457-2471.
Yuan, H., Teng, J.G., Seracino, R., Wu, Z.S. and Yao, J. (2005), "Full-range behavior of FRP-to-concrete bonded joints", *Eng. Struct.*, **26**, 553-565.
William, K.J. and Warnke, E.P. (1974), "Constitutive model for the triaxial behavior of concrete", *IABSE Report No.19*, **19**, 1-30.

NB

Notations

b_{CFRP} : Width of CFRP strip
E_c : Modulus of elasticity
f_y : Tensile strength of CFRP
f_t : Tensile strength of concrete
f_c : Compressive strength of concrete
L_{CRFP} : Length of CFRP strip
P : Applied force
P_{RXY} : Poisson ratio of CFRP
C : Cohesion
τ_{MAX} : Maximum shear strength of interface
μ : Friction coefficient